NASA CR-176995

A Reproduced Copy

OF

N86-28920

Reproduced for NASA

by the

NASA Scientific and Technical Information Facility

(NASA-CR-176995) COMPARISON OF THEORETICAL AND FLIGHT-MEASURED LOCAL FLOW AERODYNAMICS FOR A LOW-ASPECT-RATIO FIN Final Report, 31 Oct. 1980 - 31 Oct. 1984 (California Polytechnic State Univ.) 30 p CSCL 01A G3/02

N86-28920

Unclas 43347

COMPARISON OF THEORETICAL AND FLIGHT-MEASURED LOCAL FLOW AERODYNAMICS FOR A LOW-ASPECT-RATIO FIN

FINAL REPORT

PRINCIPAL INVESTIGATORS

J. Blair Johnson

Doral R. Sandlin

10/31/80 - 10/31/84

California Polytechnic State University

Aeronautical Engineering Department

San Luis Obispo, California

Grant No. NCC 4-1

Abstract

Flight test and theoretical aerodynamic data were obtained for a flight test fixture mounted on the underside of an F-104G aircraft. The theoretical data were generated using two codes, a two-dimensional transonic code called Code H, and a three-dimensional subsonic and supersonic code called wing-body. Pressure distributions generated by the codes for the flight test fixture as well as boundary layer displacement thickness generated by the two-dimensional code were compared to the flight test data. The two-dimensional code pressure distributions compared well except at the minimum pressure point and trailing edge. Shock locations compared well except at high transonic speeds. The three-dimensional code pressure distributions compared well except at the trailing edge of the flight test fixture. The two-dimensional code does not predict displacement thickness of the flight test fixture well.

CONTENTS

INTRODUCTION

The use of theoretical prediction techniques can be a useful tool in most engineering applications. In the case of aerodynamics, many computer codes exist that aid the engineer with the design and analysis of aircraft and aircraft components. Two commonly used codes are a two-dimensional transonic analysis code developed by Bauer, Garabedian, Jameson, and Korn described in reference 1, and a three-dimensional subsonic and supersonic wing-body analysis code developed by Frank Woodward and described in reference 2. Both analysis codes have been used successfully in predicting parameters for specific shapes. For example, the two dimensional code, hereafter referred to as Code H, has been used successfully for the prediction of supercritical airfoil characteristics and the three-dimensional code, hereafter referred to as the wing-body code, has been used successfully to predict the characteristics of various wing fuselage configurations.

Wind tunnel tests are frequently used as a means of obtaining experimental data. However, the data obtained in such tests in most cases must be corrected in order to obtain the results valid for flight vehicles. Such limitations as scale effects due to Reynolds number, size limitations for models or test specimens due to test section dimension, improper scaling of noise or turbulence levels in the wind tunnel, and unreliable data near a Mach number of 1.0 due to problems such as shock reflections off of the tunnel walls must be considered when conducting wind tunnel tests. The Dryden Flight Research Facility has developed an instrumented flight test fixture

(FTF) that can be attached to the underside of an F-104G aircraft and used as a "flying wind tunnel". The FTF is essentially a low aspect ratio fin incorporating a wedge-shaped airfoil.

A need exists to (1) verify Code H in order to see if it will accurately predict the aerodynamic parameters for shapes that differ from those for which it was developed, and (2) find an aerodynamic code which will predict the aerodynamic parameters for the shape used on the flight test fixture. The purpose of this study was to determine if these two codes could be used to successfully predict aerodynamic parameters for the FTF. In order to make this determination, the instrumented FTF was attached to the underside of an F-104G aircraft and flight data was obtained. At Mach numbers of 0.6, 0.7, 0.8, 0.85, and 0.9, pressure distributions and boundary layer displacement thicknesses were determined from the flight test data, and were compared to the predicted values obtained using Code H. Pressure distributions at Mach numbers between 0.6 and 1.4 were made and compared to those predicted using the wing-body code.

SYMBOLS

C_p	pressure coefficient
c	local streamwise chord of wing panel, cm
M	free-stream Mach number
p	static pressure, N/M^2
q	free-stream dynamic pressure, $0.7\ M^2p$, N/m^2
R	Reynolds number

x/c	ratio of distance from leading edge to local chord length
α	angle of attack, deg
β	angle of sideslip, deg
δ^*	boundary layer displacement thickness, cm
θ	boundary layer momentum thickness, cm

FACILITY DESCRIPTION

Flight Test Fixture

The FTF is a low-aspect ratio, fin-like shape and is mounted on the underside of an F-104G aircraft. It is oriented so that the longitudinal axis is aligned on the aircraft's lower fuselage center line (see fig. 1). It is made primarily of aluminum and weighs approximately 136 kg (300 lbs), has a chord length of 203 cm (80 in), a span of 61 cm (24 in), and a constant thickness of 16.3 cm (6.4 in) except for the forebody (see fig. 2). Two options are available for forebody shapes: (1) the basic FTF shape with a sharp leading edge (wedge forebody), and (2) the radiused forebody incorporating the front portion of a symmetrical supercritical airfoil. Only the wedged forebody was used in this study. The fin has its own air data system which consists of a pitot static probe that is mounted on a boom extending forward from the FTF. The probe is used to measure Mach number, altitude, and dynamic pressure. The FTF is equipped with flush static pressure orifices for measurements of chordwise and spanwise pressure distributions, and boundary layer rakes for measurement of

the boundary layer velocity profile. For this study, 20 static orifices were used located on both sides of the FTF as shown in figure 3. Sixteen of the orifices were placed along the chord at approximately the 50% span position. Four orifices were located along a spanwise direction shown in figure 3 for the purpose of determining spanwise flow conditions. The boundary layer rakes were mounted on both sides of the FTF at the approximately 90% chord and 50% semispan positions.

A pulse code modulation (PCM) system is used for data acquisition. Data from the PCM, which is capable of multiplexing 40 channels at a maximum frequency of 80 Hz, is both transmitted to the ground via telemetry and recorded on board. All pressure measurements were obtained by a 48-port scanivalve and two other individual differential pressure transducers. The pressures measured by the scanivalve and transducers were referenced to the FTF boom-static pressure.

The F-104G aircraft has its own independent instrument system and an aircraft flight trajectory guidance system. The trajectory guidance system uplinks engineering parameters calculated on a ground based computer to a cockpit display in real time. From this display, bank error during constant Mach, α and altitude turns, Reynolds number error, sideslip error, and Mach number error can be determined in real time by the pilot. A more complete description of the FTF is available in reference 3.

ANALYSIS CODE DESCRIPTION

Code H

Francis Bauer, Paul Garabedian, David Korn, and Anthony Jameson from the Courant Institute of Mathematical Sciences of New York University, have developed a technique of computing supercritical airfoil sections and determining the off-design flow conditions. The equations of motion used in this method are the equations of potential flow. The flow is assumed to be transonic, steady, irrotational, inviscid, compressible, and two-dimensional. Instead of solving the problem of computing shock free transonic flow past a given profile, the inverse problem was solved. That is, they assumed smooth transonic flow and then found the body which generated it. This approach was taken in order to eliminate certain mathematical difficulties. The problem was formulated by writing the equations of motion of the inverse problem in matrix form, extending all of the variables into the complex domain, and introducing characteristic coordinates and then expressing the equations of motion in characteristic form. A treatment of compressibility is made by combining a regular solution with a singular solution that is related to the fundamental solution in the hodograph plane. The formulated equations are solved numerically using a finite difference scheme. Not only was the

inverse problem of determining a shape that would result in the smooth transonic flow treated, the off-design conditions (at different angles of attack and free-stream velocity) were also solved. The result was several computer programs which were designated Programs A through E. A description of the theory and programs is available in reference 1.

The authors of these programs have modified and improved their original work by introducing a better model of the trailing edge, and using a rotated finite different scheme that enables them to use an arbitrary curvalinear coordinate system. The use of an arbitrary curvalinear coordinate system permits the handling of supersonic and subsonic free-stream Mach numbers and the capturing of shock waves as far back on the airfoil as desired. The turbulent boundary layer is treated using a semi-empirical method and the effects of displacement thickness on airfoil shape is accounted for. Shock waves are handled by calculating weak solutions to the applicable partial differential equations that include one or more shock waves that satisfy an entropy inequality. These modifications are included in a new program designated Code H. A description of this program can be found in reference 1. The author claims these programs provide a physically adequate computer simulation of the compressible potential problems of transonic flow for a smooth 2D shape.

The Wing-Body Code

The Boeing Company under contract with NASA/Ames Research Center has developed a three-dimensional wing-body constant pressure panel

code for subsonic and supersonic potential flows. The program calculates steady pressure distributions on wing and wing-body combinations of arbitrary plan form in subsonic and supersonic flow. The surface pressures are integrated to give the lift, drag, and pitching moment. The yawing and rolling moments and the side force can be determined for unsymmetrical configurations; however, for this study, only the pressure coefficients that were predicted for the surface of the flight test fixture were used. In addition, the original version of the Ames wing-body code was modified by personnel at Ames and an updated version of this program was made available to NASA's Dryden Flight Research Facility for use in this study.

The method divides the wing-body combination or wing alone into numerous constant pressure panels. A constant source distribution is used in the body panels and a vortex distribution is used in the wing and tail panels. The code arrives at analytical expressions for the perterbation velocities induced at each panel. Then, the pressure coefficient at the panel control points are calculated in terms of the perterbation velocities. The forces and moments acting on the wing-body combination can be calculated by using a numerical integrating scheme.

A further description as well as previous utilization of the code at the Dryden Flight Research Facility is given in reference 4.

MODELING OF THE FLIGHT TEST FIXTURE

Code H Modeling

In all cases presented, the code was run using 0° angle of attack, and four smoothing iterations of the FTF coordinates were made before the aerodynamic shape was conformly mapped into the unit circle. The circle was overlayed with both a crude grid of 80 × 15 mesh intervals and a finer grid of 160 × 30 mesh intervals in the angular and radial directions. Flow calculations and boundary layer corrections were computed for a maximum of 20 cycles on the crude grid, and a maximum of 10 cycles on the finer grid. The convergence tolerance, a tolerance of the maximum velocity potential and the maximum circulation corrections, was set at 5×10^{-6}. The program was run until the convergence tolerance was achieved. The boundary layer correction option of the code was used, and the transition was set at the 7.5% chord position. To utilize this option, a Reynolds number must also be specified. In this case, Reynolds numbers of 2×10^6 and 14×10^6 were used.

The FTF was first modeled using 46 upper and 46 lower surface points with a high density of points at the wedge corner of the FTF located at the approximate 17% chord postion. Because of the discontinuity at the corners, the code would not complete the run. Next, a model with 46 upper and 46 lower surface points was attempted but the sharp corners of the wedge were radiused and the coordinates were run

through a separate smoothing program before being entered into the two-dimensional code. Figure 4 shows a comparison at this model shape to the actual shape of the FTF. A comparison of the predicted and experimental pressure distribution is shown in figure 5 for the 0.7 Mach case. This figure shows that the code predicted pressure distribution appears to predict pressure coefficient levels well; however, there is a difference of approximately 7% chord in the chordwise location of the peak values of pressure coefficients. In addition, the experimental data indicates a trend of decreasing pressure at the trailing edge of the FTF that is not predicted by the code. The variation of the peak pressure coefficient positions between the experimental and the computer predicted data were believed to be caused by the variation of shape of the actual and computer models.

In order to test this hypothesis, a model consisting of 16 upper and 16 lower surface points was run. The model having fewer points allowed the smoothing subroutine internal to the code to have a greater effect, as shown in figure 6. The shape of the model is very similar to the actual FTF. Figure 7 shows good correspondence for the positions of the minimum pressure coefficients determined from experimental and theoretical data. The noted lack of correspondence of pressure coeffficients at the trailing edge was not believed to be caused by modeling and will be discussed in the RESULTS AND DISCUSSION section of this report.

Wing-Body Code Modeling

Since this code is three dimensional, it is necessary to not only model the FTF but also the F-104G aircraft. The wing-body code allows for a maximum of 100 wing and 100 body panels. These panels were divided between the fuselage of the F-104G and the wing and FTF. The fuselage was modeled with 96 panels and the wing and the FTF used 82 panels. Thirty-two panels were used for the F-104G wings, and 50 panels were used for the FTF. Figure 8 shows the panel breakdown of the F-104G and the FTF. The F-104G was modeled as a cylinder with a radius of 80 cm and a length of 1160 cm, and a conical nose of 470 cm in length. The wings of the F-104G were modeled as a bi-convex surface with a thickness ratio of 3.36%, a semispan length of 230 cm, a sweep back of the quarter chord of 18.6°, and an anhedral of 10°. The vertical and horizontal stabilizers were not included in the model in order to allow a greater number of panels for the FTF.

DISCUSSION AND RESULTS

Code H Pressure Distributions

Figures 9(a), 9(b), 9(c), and 9(d) present pressure distributions for the FTF using experimentally and theoretically determined data for Mach numbers of 0.7, 0.8, 0.85, and 0.9. The experimental data is based on Mach numbers measured with the FTF noseboom since only the FTF was modeled in this case. Code H was used

to calculate the theoretically determined pressure coefficients. As shown in figure 9(a) where the Mach number is 0.7, the flow accelerates and the pressure coefficient drops from the nose to about the point on the surface where the discontinuity occurs (approximately 17% chord). Beyond this point the flow slows as it changes direction and the pressure coefficient increases. There is good correspondence between the experimental and theoretical data with good correspondence between the experimental and theoretical data with the exception of the peak minimum values of pressure coefficients. Code H predicts higher minimum pressure coefficients than are obtained from the flight test data. No shock exists for this Mach number, since supersonic flow velocities do not occur on the FTF.

Figures 9(b) through 9(d) show data for Mach numbers of 0.8, 0.85, and 0.9. For these Mach numbers the flow accelerates from the nose to the surface discontinuity, and reaches sonic condition. As the flow turns through an angle of approximately 13.05° (one-half the wedge angle) at the discontinuity point, it accelerates, reaching a peak value and goes through a normal shock. The shock causes a rapid increase in pressure coefficient and a slowing of the flow to sonic velocities. These figures reveal that a fairly good correspondence between experimental and theoretical data exists; however, the peak minimum values of pressure coefficients differ, and as the Mach number increases from 0.8 to 0.85 the predicted shock location tends to shift beyond the 20% chord position. At 0.9. Mach number, the shock has shifted to about the 50% chord position in the theoretical

data. The shock remains near the 20% chord position for all Mach numbers for the experimental data. We can conclude that Code H does not accurately predict shock location for the wedge shaped FTF near Mach 1 or high transonic speeds.

At approximately the 70% chord position on the FTF, the two curves deviate and the experimental data reveal a decreasing pressure that the theoretical method does not predict. A possible explanation of why the two curves deviate near the trailing edge follows; the FTF can be considered to be an aft-facing step of height equal to one-half the width of the FTF, and flight measured pressure characteristics of aft-facing steps presented in reference 5 indicate that the base pressure does indeed have an effect on the pressure measured upstream of the aft-facing step. But the code does not account for this because a trailing edge of finite thickness is advanced linearly until is closes or exceeds chord length, whichever occurs first. Therefore, an attempt was made to alter the trailing edge of the FTF model. The model was geometrically scaled down and a boattail was added in order to effectively accelerate the flow at points near the trailing edge.

The pressure distribution for the boattail FTF in figure 10 shows that decreasing pressure at the tailing edge is evident but not nearly of sufficient quantity to match the experimental data. The boattail of greater curvature was attempted, but the code would not run because points spaced too closely together at the trailing edge led to computational difficulties. Even with fewer points at the trailing edge, a run could not be completed because of the amount of curvature needed to simulate the flow at the trailing edge.

The Wing-Body Pressure Distributions

The wing-body code was run for the F-104G/FTF model at 0.6, 0.7, 0.8, 0.9, 1.2, and 1.4 Mach numbers. Angles of attack of 0^{o}, 2^{o} and 4^{o} were used for the 0.6 and 1.4 Mach number cases. These two cases which are the extremes of the Mach number range tested were run at different angles of attack to determine the effects of aircraft angle of attack on the data. Figures 11(a) and 11(f) show data for these cases with the wing-body code data for the three angles of attack and the flight test superimposed. Little difference exists for the three sets of angle of attack data. The data varies little with angle of attack. Therefore, the Mach number cases of 0.7, 0.8, 0.9 and 1.2 were run at 2^{o} angle of attack which approximates the F-104's angle of attack during the test flights. All cases were run at 0^{o} sideslip angle and the flight test data were recorded at very small sideslip angles. The pressure coefficients given in the output of the wing-body code act at the centroid of the panel and represent the average pressure over the panel. Since the wing-body code is three dimensional and the model includes the aircraft, the flight test data were based on at Mach numbers measured by the aircraft instrumentation system instead of the flight test fixture's air data system.

Figures 11(a) and 11(b) depict data for Mach numbers of 0.6 and 0.7. These figures reveal an accelerating flow from the nose of the flight test fixture to the surface discontinuity and a slowing of the flow aft of the forebody with an accompanying increase of pressure coefficient. There is a fairly good match of the flight test and

theoretically predicted data. The peak negative pressure coefficient for the flight test data is more negative than the predicted value, the predicted values of pressure coefficient are generally higher than values determined from flight test data, and the trend of decreasing pressure coefficients exists near the trailing edge of the flight test fixture for the flight test data that is not present for the theoretically predicted data.

Figures 11(c) and 11(d) show data for the other two subsonic cases of 0.8 and 0.9 Mach numbers. As discussed earlier, at these flight speeds the flow is accelerated by the forebody to supersonic speeds and a normal shock wave forms. These shock waves are evident in the flight test data for Mach numbers of 0.8 and 0.9. While the shock waves are not predicted by the wing-body code, the point of minimum pressure coefficient does occur at the 20% chord position for both sets of data. This method is no capable of transonic shock wave prediction. In addition, the data indicate an inability of the wing-body code to predict the decreasing values of pressure coefficient near the trailing edge of the FTF for similar reasons as Code H results. However, for the 0.9 Mach number case the two sets of data correspond very well over a large range of chord positions.

The data for the supersonic Mach number cases of 1.2 and 1.4 Mach number are shown in figures 11(e) and 11(f). For both cases the flow over the FTF is subsonic since the one-half wedge angle of approximately 13.05° is large enough to cause the shock to detach from the nose.

The portion of the shock forward of the nose is normal and the normal shock wave creates subsonic flow over the nose of the FTF and large positive pressure coefficients. The flow accelerates over the forebody, does not reach sonic conditions, and decelerates from the surface discontinuity to the trailing edge. The two sets of data match very well over the entire FTF; however, in the 1.2 Mach number case, the theoretical data reflects very sharp changes of pressure coefficient about the 50% chord position. It is possible that the wing-body code is introducing fuselage effects that do not occur in the experimental data at this particular Mach number. To check this possibility, the FTF was modeled excluding the F-104G aircraft. Figure 12 shows that the pressure distribution smooths out and compares well to the experimental data, suggesting that the code was indeed introducing inaccurate fuselage effects.

It is interesting to note that the trailing edge divergence noted in the subsonic data changes for the supersonic data. The experimental data indicate an increasing and then decreasing trend of pressure coefficients near the trailing edge of the FTF.

Displacement Thickness Distribution

Code H provides a semi-empirical turbulent boundary-layer correction in the transonic flow analysis. Displacement thickness (δ^*) is calculated by relating momentum thickness and shape factor where momentum thickness is determined using Von Karman's equation and the

shape factor is determined semi-empirically. Because the laminar portion of the boundary layer is considerably smaller than the turbulent portion, it is not considered in the boundary-layer correction calculations. For the boundary-layer correction, a transition point must be specified. A transition location of 7.5% chord was used in all cases. This most closely approximated where transition was thought to occur.

In figure 13, experimental and theoretical displacement thickness at 85% chord are plotted vs Mach number. Reynolds numbers of 2×10^6 and 14×10^6 were used. The shapes of the curve agree but they are displaced. Also, the experimental data with approximate Reynolds numbers of 20×10^6 was quite scattered around 0.8 Mach. This scatter in the experimental data is probably caused in part by separated flow due to a shock wave that is reattaching. We can conclude from the data shown in figure 13 that the semi-empirical boundary layer used in Code H does not permit precise determination of the displacement thickness for the FTF with the wedge shaped nose.

CONCLUSIONS

An F-104G aircraft with an attached FTF with a wedged shaped forebody has been tested at NASA/Dryden Flight Research Facility. Pressure distributions and displacement thicknesses have been determined from the flight test data. Two theoretical prediction methods have been used to predict similar data for the FTF at the flight test speeds. One is a two-dimensional method and has been designated Code H by Bauer, et al, who are the authors of this method. The other

is a three-dimensional method and has been designated as the wing-body code by its author, Frank Woodward. The results obtained from the comparison of flight test data with the data predicted by the codes follows.

Code H Comparisons

(1) For subsonic flight speeds and flow over the FTF, Code H adequately predicts values of pressure coefficients except at the minimum pressure point and at the trailing edge. Code H predicts higher values at the minimum pressure point and the experimental data reveal an increasing pressure coefficient that Code H does not predict.

(2) For subsonic flight speeds and supersonic flow at some point on the FTF, the shock wave that forms is located at the approximate 20% chord position. Code H predicts a shifting position of the shock waves with increasing speed and does not adequately predict the increasing pressure coefficient divergence at the trailing edge of the FTF. Otherwise Code H adequately predicts the level of the pressure coefficients at other positions on the FTF.

Wing-Body Code Comparisons

(1) For subsonic speeds and flow over the FTF, the wing-body code adequately predicts levels of pressure coefficients except at the trailing edge. The decreasing pressure coefficient divergence at the trailing edge is not predicted by the wing-body code.

(2) For subsonic flight speeds and supersonic flow at some point on the FTF, the wing-body code which is incapable of shock wave prediction adequately predicts pressure coefficient levels except at the trailing edge and at the minimum pressure point.

(3) For supersonic flight speeds and subsonic flow over the FTF the wing-body code adequately predicts levels of pressure coefficients.

Displacement Thickness Comparisons

The semi-empirical boundary layer used in Code H does not precisely predict the displacement thickness of the FTF for the two Reynolds numbers tested.

REFERENCES

1. Korn, David; Jameson, Anthony; Garabedian, Paul R.; and Bauer, Frances: "Supercritical Wing Sections II: A Handbook," Springer-Verlag, Berlin-New York, 1975.

2. Woodward, Frank A.: "Analysis and Design of Wing-Body Combinations at Subsonic and Supersonic Speeds," J. Aircraft, Vol. 5, no. 6, pp. 528-534, Nov. - Dec. 1968.

3. Meyer, Robert, Jr.: "Unique Flight Test Facility: Description and Results," ICAS-82-5.33.

4. Curry, Robert E.: Utilization of the Wing-Body Aerodynamic Analysis Program," NASA TM-72856, October 1978.

5. Powers, Sherylla Goecke: Flight Measure Pressure Characteristics of Aft-Facing Steps in Thick Boundary Layer Flow for Transonic and Supersonic Mach Numbers," NASA CP-2054, Vol. I, September, 1978.

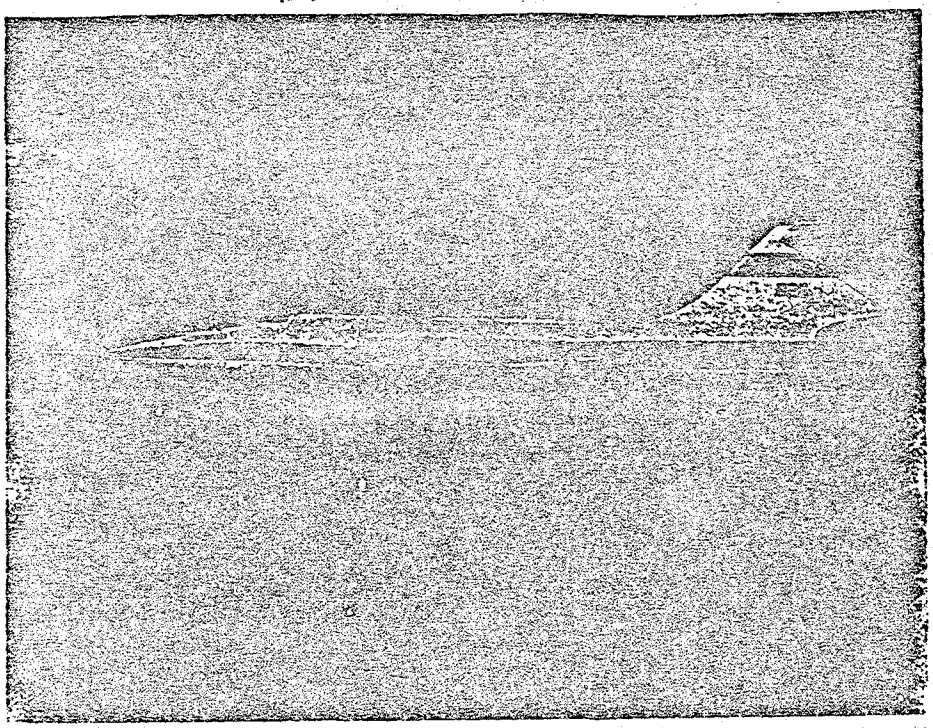

Fig. 1 Flight test fixture installed on lower fuselage of F-104 carrier aircraft.

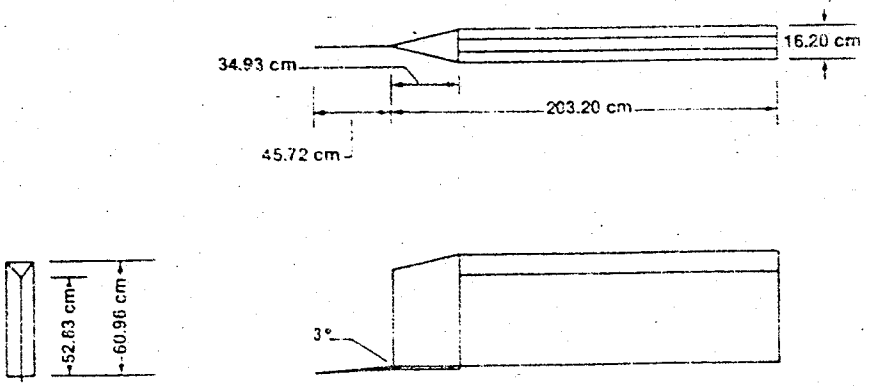

Fig. 2 Three view drawing of flight test fixture.

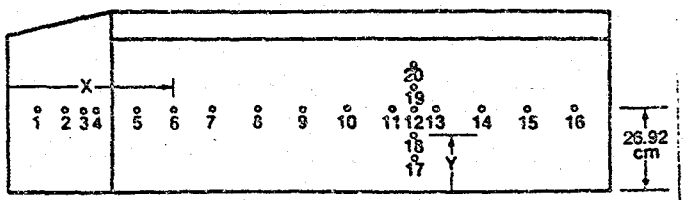

	X, in	cm
1	3.75	9.53
2	7.50	19.05
3	9.50	24.00
4	11.50	29.21
5	17.00	43.18
6	22.00	55.88
7	27.00	68.58
8	33.00	83.82
9	39.00	99.06
10	45.00	114.30

	X, in	cm
11	51.0	129.54
12	54.0	137.16
13	57.0	144.78
14	63.0	160.02
15	69.0	175.26
16	75.0	190.50
	Y, in	cm
17	4.60	11.68
18	7.0	18.30
19	13.5	34.29
20	16.5	41.91

* Orifice 3 is on right side only
numbers 1,2,4 on right and left side

Fig. 3 Orifice location for flight test fixture.

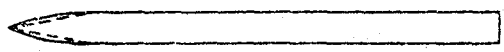

Fig. 4 Comparison of radiused-nose model shape to actual shape of the FTF.

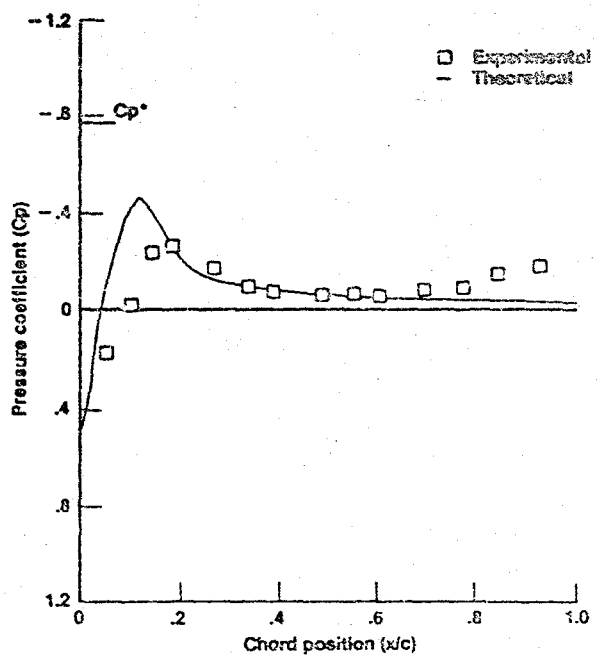

Fig. 5 Pressure distribution generated by code H for a 92 point model of the FTF. M=0.7.

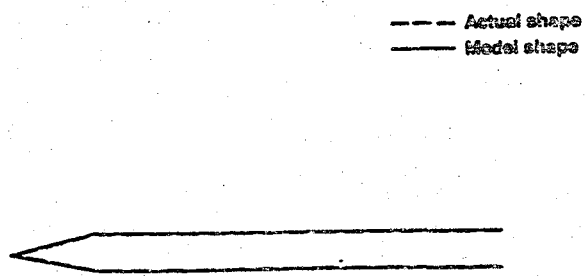

Fig. 6 Comparison of 32 point model to actual shape of the FTF.

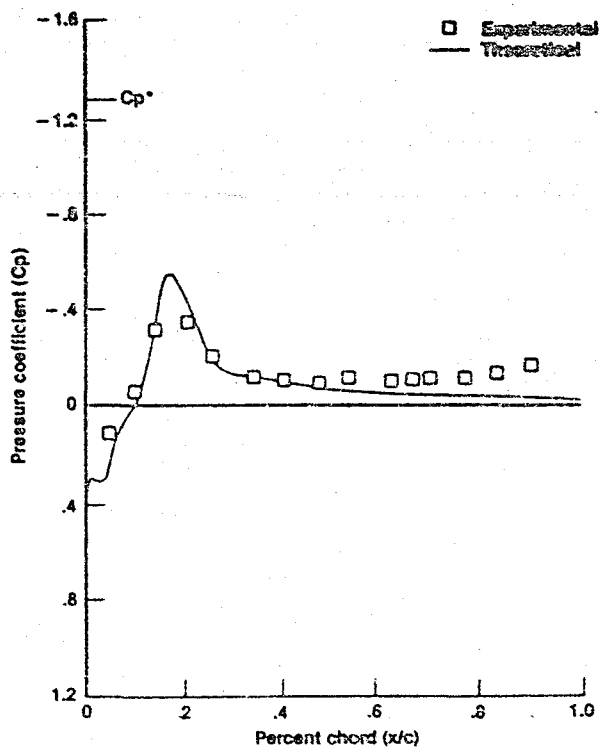

Fig. 7 Pressure distribution generated by code H for 32 point model of FTF. M=0.6.

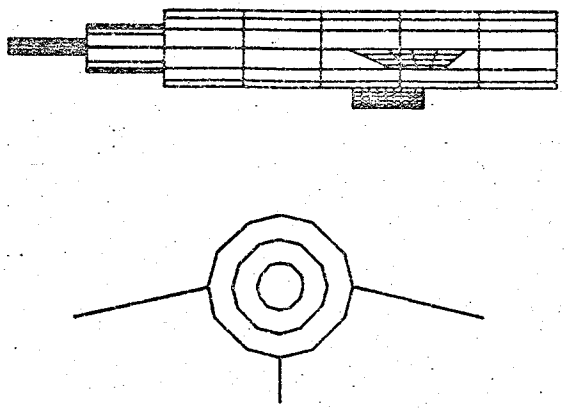

Fig. 8 Panel break-down of F-104/FTF model used for a wing-body code.

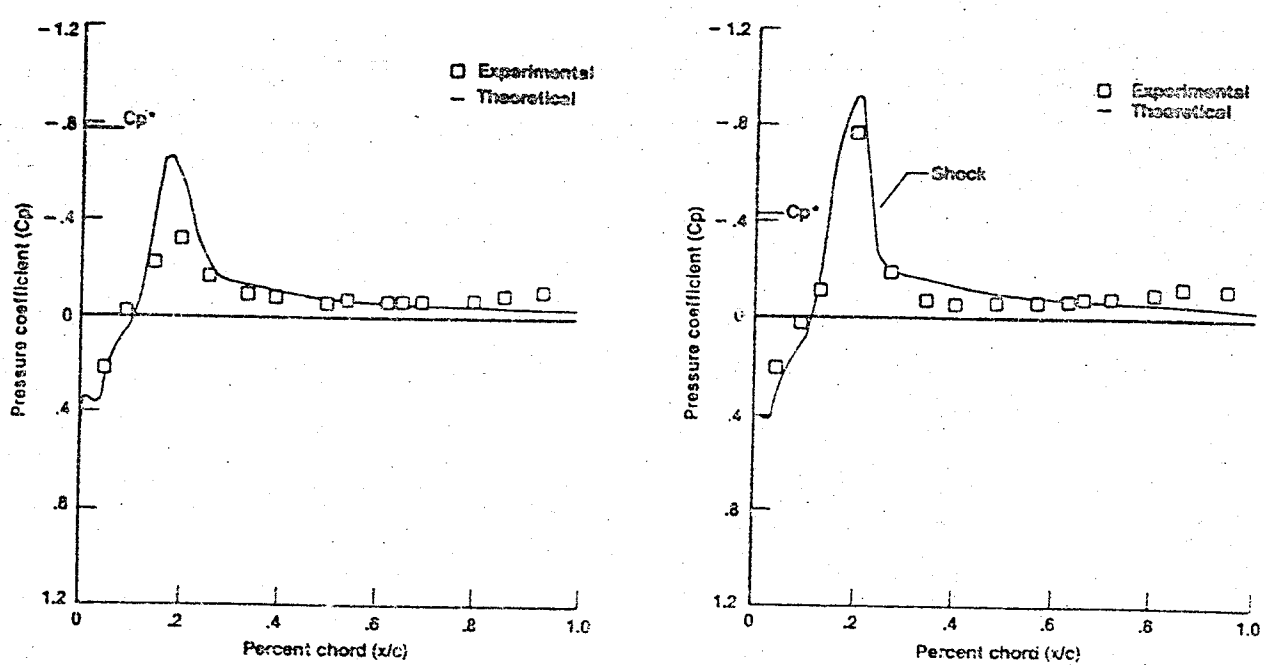

(a) M=0.7.

(b) M=0.8.

Fig. 9 Pressure distribution generated using code H.

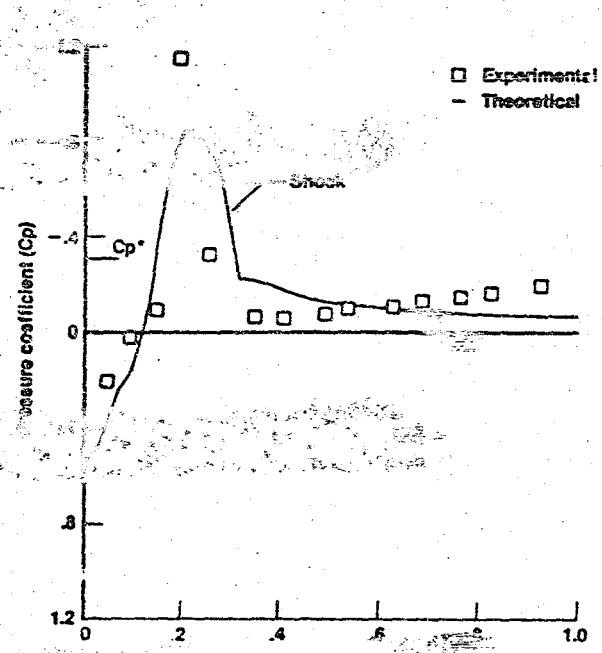

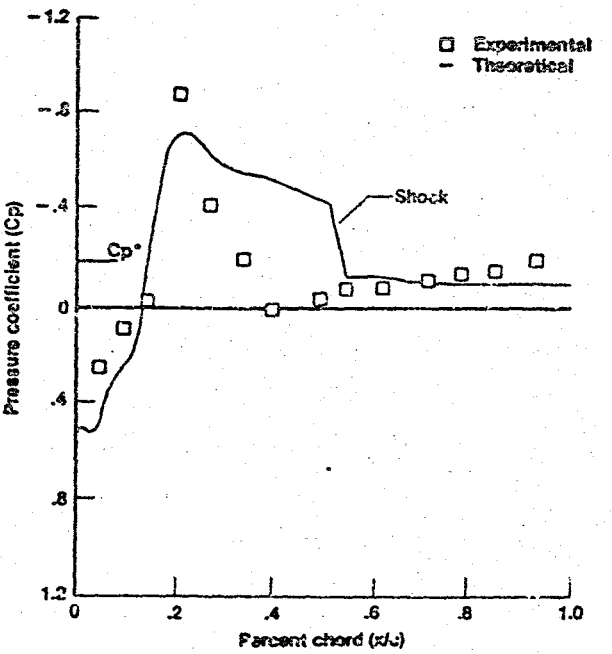

(d) M=C.9.

Fig. 9 concluded.

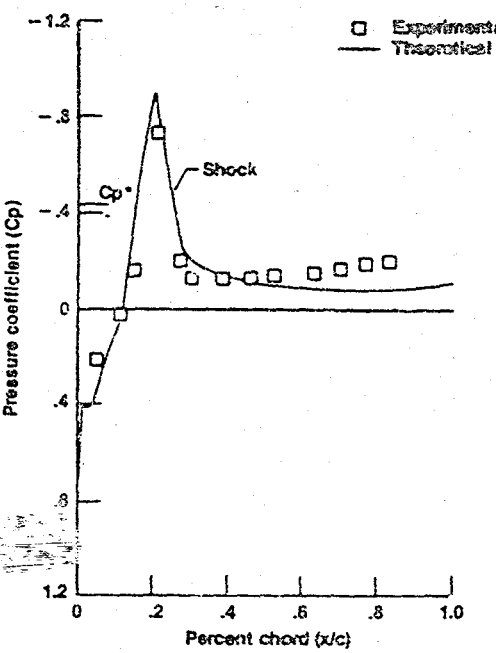

Fig. 10 Pressure distribution generated by code H for boattail model of FTF. M=0.8.

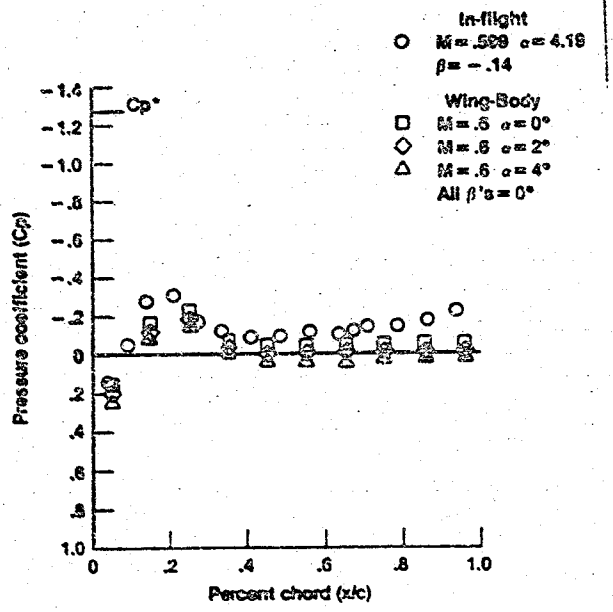

(a) M=0.6.

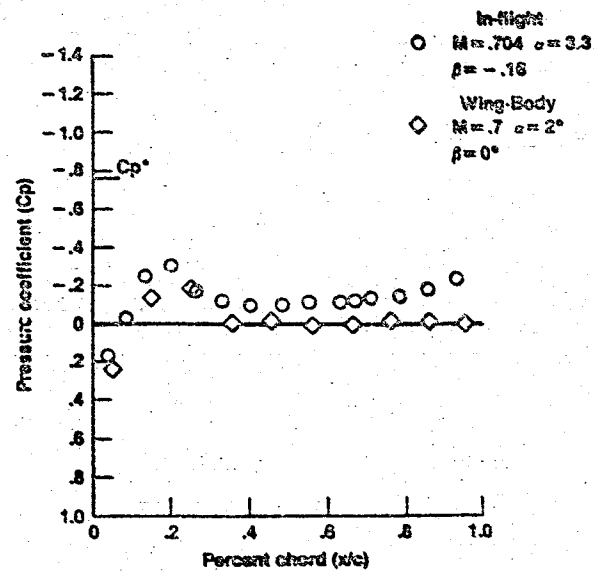

(b) M=0.7.

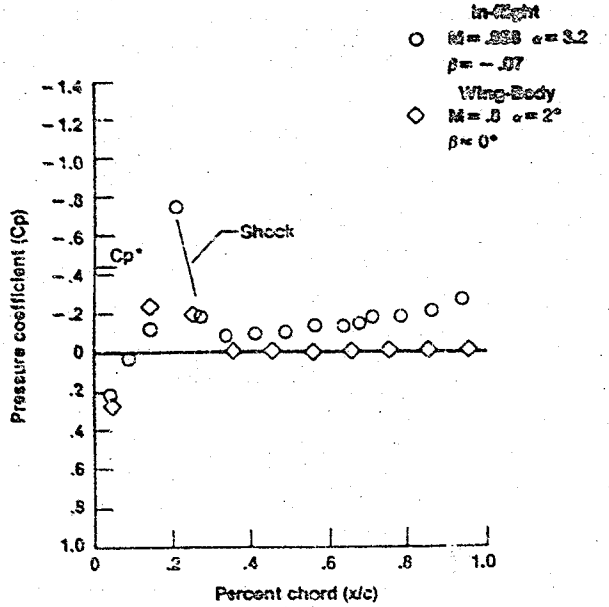

(c) M=0.8.

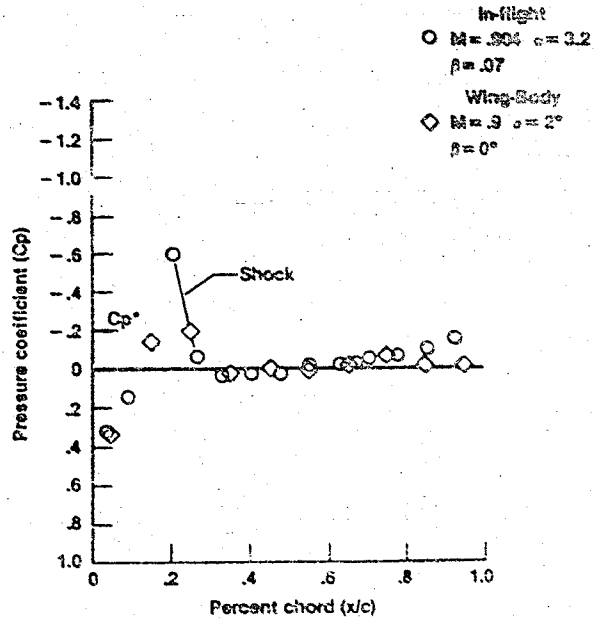

(d) M=0.9.

Fig. 11 Pressure distribution generated by wing-body code.

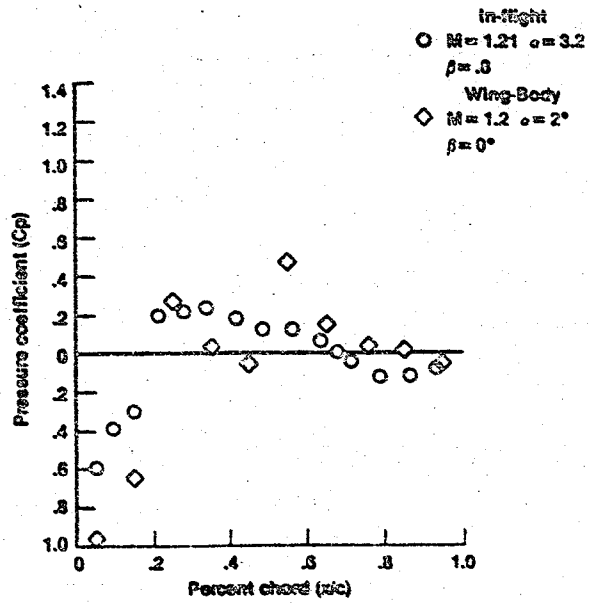

(e) M=1.2.

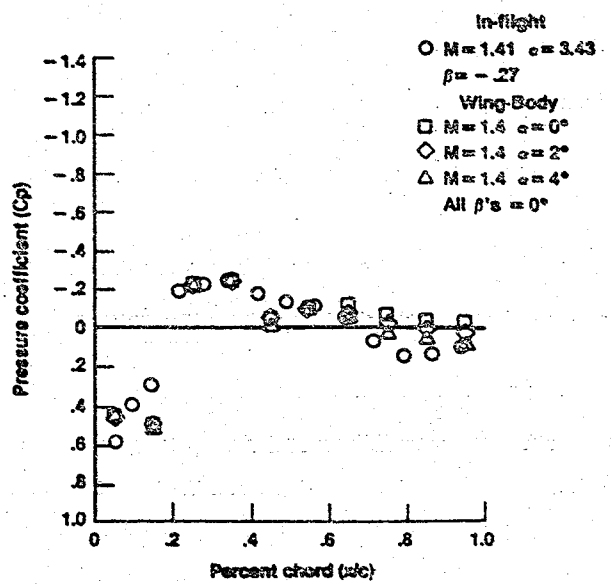

(f) M=1.4.

Fig. 11 concluded.

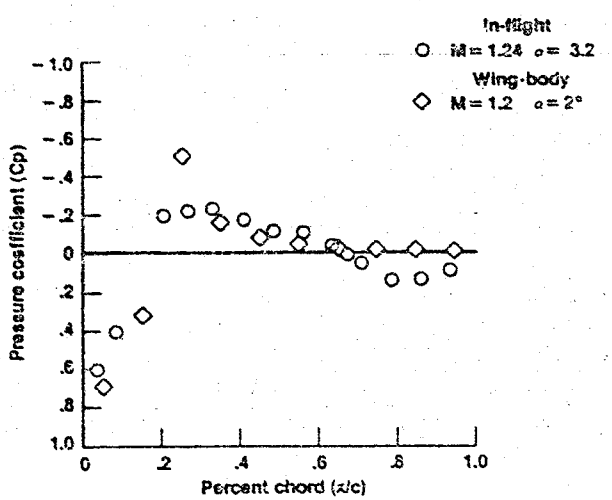

Fig. 12 Pressure distribution generated by wing-body code for isolated FTF model.

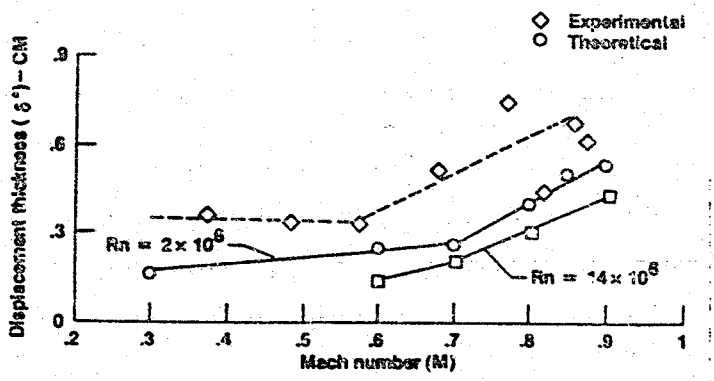

Fig. 13 Displacement thickness generated by code H as a function of Mach number.

End of Document